UNIVERSITY OF COPENHAGEN

Induction of quiescence (G0) in bone marrow stromal stem cells enhances their stem cell characteristics

Rumman, Mohammad; Majumder, Abhijit; Harkness, Linda; Venugopal, Balu; Vinay, M. B.; Pillai, Malini S.; Kassem, Moustapha; Dhawan, Jyotsna

Published in:
Stem Cell Research

DOI:
10.1016/j.scr.2018.05.010

Publication date:
2018

Document version
Publisher's PDF, also known as Version of record

Document license:
CC BY-NC-ND

Citation for published version (APA):
Rumman, M., Majumder, A., Harkness, L., Venugopal, B., Vinay, M. B., Pillai, M. S., Kassem, M., & Dhawan, J. (2018). Induction of quiescence (G0) in bone marrow stromal stem cells enhances their stem cell characteristics. *Stem Cell Research*, *30*, 69-80. https://doi.org/10.1016/j.scr.2018.05.010

Download date: 05. May. 2023

Stem Cell Research 30 (2018) 69–80

Contents lists available at ScienceDirect

Stem Cell Research

journal homepage: www.elsevier.com/locate/scr

Induction of quiescence (G0) in bone marrow stromal stem cells enhances their stem cell characteristics

Mohammad Rumman[a,b,c,1], Abhijit Majumder[a,d,1], Linda Harkness[c,1,2], Balu Venugopal[a,3], Vinay M.B.[a,4], Malini S. Pillai[a], Moustapha Kassem[c,e,f,*], Jyotsna Dhawan[a,g,**]

[a] Institute for Stem Cell Biology and Regenerative Medicine (inStem), Bengaluru 560065, India
[b] Manipal Academy of Higher Education, Manipal, Karnataka, India
[c] Laboratory for Molecular Endocrinology (KMEB), Department of Endocrinology and Metabolism, University Hospital of Odense, Odense, Denmark
[d] Indian Institute of Technology-Bombay (IITB), Mumbai, India
[e] Department of Cellular and Molecular Medicine, Danish Stem Cell Center (DanStem), University of Copenhagen, Copenhagen, Denmark
[f] Stem Cell Unit, Department of Anatomy, Faculty of Medicine, King Saud University, Saudi Arabia
[g] CSIR-Centre for Cellular and Molecular Biology, Hyderabad, 500 007, India

ARTICLE INFO

Keywords:
Quiescence (G0)
BMSC
Transcriptome
Suspension culture
Adhesion
Substrate stiffness
Cell cycle
Osteoblastic differentiation
Reprogramming

ABSTRACT

Several studies have suggested that bone marrow stromal steam cells (BMSC) exist in a quiescent state (G0) within the in vivo niche; however, an explicit analysis of the biology of G0 state-BMSC has not been reported. We hypothesized that induction of G0 in BMSC might enhance their stem cell properties. Thus, we induced quiescence in BMSC in vitro by (a) suspension culture in a viscous medium or (b) culture on soft polyacrylamide substrate; and examined their molecular and functional phenotype. Induction of G0 was confirmed by bromodeoxyuridine (BrdU) labelling and analysis of cell cycle gene expression. Upon reactivation and re-entry into cell cycle, G0 state-BMSC exhibited enhanced clonogenic self-renewal, preferential differentiation into osteoblastic rather than adipocytic cells and increased ectopic bone formation when implanted subcutaneously in vivo in immune-deficient mice, compared to asynchronous proliferating (pre-G0) BMSC. Global gene expression profiling revealed reprogramming of the transcriptome during G0 state including significant alterations in relevant pathways and expression of secreted factors, suggesting altered autocrine and paracrine signaling by G0 state-BMSC and a possible mechanism for enhanced bone formation. G0 state-BMSC might provide a clinically relevant model for understanding the in vivo biology of BMSC.

1. Introduction

Cellular quiescence (G0) is an intrinsic property of adult stem cells (ASC) in vivo that allows suppression of cell division and tissue-specific genetic programs without affecting the capacity for cell cycle re-entry and subsequent differentiation (Cheung and Rando, 2013, Subramaniam et al., 2013, Rumman et al., 2015). Earlier studies demonstrated that bone marrow stromal cells (BMSC) in vivo display characteristics of G0 state, as they are label-retaining and resistant to 5-fluorouracil (5-FU)-induced apoptosis (Haas et al., 1969). More recently, a subset of label-retaining cells was identified in mouse periosteum and found to co-express BMSC markers (Cherry et al., 2014). In addition, subpopulation of freshly isolated PDGFRα(+) SCA-1(+) murine BMSC were found to be in G0 state as assessed by DNA and RNA content (Morikawa et al., 2009). However, information regarding the functional characteristics of G0 BMSC has not been reported.

BMSC (also known as bone marrow skeletal stem cells or mesenchymal stem cells) represent a population of plastic adherent cells isolated from bone marrow aspirates (Zaher et al., 2014, Bianco and Robey, 2015) and exhibit regeneration-enhancing characteristics upon transplantation in a number of in vivo disease models such as bone

* Correspondence to: M. Kassem, Laboratory for Molecular Endocrinology (KMEB), Department of Endocrinology and Metabolism, University Hospital of Odense, Odense, Denmark.
** Correspondence to: J. Dhawan, Institute for Stem Cell Biology and Regenerative Medicine, National Center for Biological Sciences, GKVK Campus, Bellary Road, Bengaluru 560065, India.
E-mail addresses: mkassem@health.sdu.dk (M. Kassem), jdhawan@instem.res.in (J. Dhawan).
[1] Equal contribution.
[2] Current addresses: Austrialian Institute of Bioengineering and Nanotechnology (AIBN), University of Queensland, St Lucia, Queensland.
[3] Current addresses: Sree Chitra Tirunal Institute for Medical Sciences and Technology Tiruvanathapuram, India.
[4] Current addresses: National University of Singapore (NUS), Singapore.

https://doi.org/10.1016/j.scr.2018.05.010
Received 1 January 2018; Received in revised form 22 April 2018; Accepted 16 May 2018
Available online 17 May 2018
1873-5061/ © 2018 Published by Elsevier B.V. This is an open access article under the CC BY-NC-ND license (http://creativecommons.org/licenses/BY-NC-ND/4.0/).

fracture (Granero-Molto et al., 2009), ischemic heart disease (Cai et al., 2016), liver injury (Wang et al., 2016). However, little is known about the biology of G0 BMSC, and many inferences are based on studies of BMSC in culture may not be appropriate since proliferating plastic-adherent cells differ in key regulatory properties from the G0 state that predominates in adult stem cells in vivo (Morikawa et al., 2009; Li et al., 2014).

As a first step in understanding the biology of quiescent BMSC, we examined the effect of inducing the G0 state on stem cell and differentiation functions in culture. In a number of cellular models, induction of G0 causes significant changes in cellular and molecular functions of the cells (Pallafacchina et al., 2010; Mourikis et al., 2012). Thus, we induced G0 in BMSC using two approaches: suspension culture in methylcellulose (MC) and culture on soft polyacrylamide (PAA) substrates and we examined the impact on BMSC stemness and changes in transcriptome as compared to cultured asynchronous proliferating (pre-G0) BMSC. Our results demonstrate that both these methods are efficient in inducing G0 state in BMSC and led to enhanced self-renewal ability, osteoblastic differentiation and ectopic bone formation upon transplantation in vivo. These changes were associated with significant changes in global gene expression inducting upregulation of intracellular signaling pathways known regulate osteoblast differentiation and bone formation. We conclude that induction of quiescence in cultured BMSC provides a useful model for analysis of mechanisms that might be relevant to the biology of BMSC in vivo.

2. Materials and methods

2.1. Cell culture

Both human and mouse cells were employed. The hBMSC-TERT cell line which is a proven model for primary hBMSC due its stable phenotype (Simonsen et al., 2002; Twine et al., 2018) was used for transcriptome analysis. Primary human and mouse BMSC were used to corroborate the results obtained in hBMSC-TERT cells (Supplementary Table 1).

Human bone marrow stromal stem cells (hBMSC) (from healthy donors) were purchased from Texas A&M Health and Science Centre (Texas, USA) and used between passages 1–3. hBMSC-TERT were derived in Prof. Moustapha Kassem's laboratory by overexpressing human TERT (*telomerase reverse transcriptase*) gene in hBMSC (Simonsen et al., 2002). Mouse bone marrow stromal stem cells (mBMSC) were isolated from 8-week old C57BL/6 mouse hind limb bones as described previous (Soleimani and Nadri, 2009). BMSC were maintained as asynchronous proliferating cultures (pre-G0) in growth medium (MEM-alpha, 10% fetal bovine serum (FBS), penstrep, glutamax) (Gibco) and passaged at 60–70% confluency. 2% methylcellulose (MC) (Sigma) stock used for suspension culture was prepared as described previously (Arora et al., 2017). To induce G0 in MC suspension culture, asynchronously proliferating (pre-G0) BMSC were trypsinized and re-suspended in MC at a density of 10^6 cells per 10 ml of suspension medium and cultured for 48 h. Briefly, for preparing 10 ml MC suspension, 10^6 cells were collected in 500 µl of growth medium in 50 ml falcon, to which was added FBS (10%), penstrep, glutamax, HEPES (10 mM, pH 7.3) and 2% MC (up to 10 ml, final MC concentration 1.3%). For reactivation studies, MC cell suspension was diluted with 40 ml PBS (pre-warmed at 37 °C), centrifuged at 1800*g* for 30 mins at room temperature without brakes, the supernatant discarded and the loose pellet dispersed by gentle pipetting. Cells were washed twice with 40 ml of warm PBS, first at 800 g for 15 min, and then at 250 g for 5 min (Arora et al., 2017). This harvest procedure yielded optimal viability. The harvested cells were counted and checked for viability using trypan blue before replating on tissue culture plastic dishes or lysed directly for RNA and protein isolation.

Polyacrylamide gels (PAA) substrates of different stiffness were prepared by cross-linking 40% PAA and 2% bis-acrylamide solution (BioRad) mixed at different concentrations in PBS, as described previously (Pelham and Wang, 1997). Details of the substrate preparation and rigidity values for different combinations of PAA and bis-acrylamide were as described (Tse and Engler, 2010). Briefly, the gels were prepared between two parallel glass cover slips, one coated with 3-APTMS ((3-aminopropyl) trimethoxysilane) (Sigma) and the other with octadecyl-trichlorosilane (Sigma), to render the cover slip respectively adherent and non-adherent to gel. Following cross-linked and gelling, the non-adherent plate was removed, and the gel was coated with type I collagen (Advanced Biomatrix) using sulfo-SANPAH (sulfosuccinimidyl 6-(4′-azido-2′-nitrophenylamino) hexanoate) based conjugation (Yeung et al., 2005) under UV for 15 min. Gels were washed with PBS and maintained under 50 µg/ml of type I collagen solution at 4 °C overnight. The control cover slip was also coated with Type 1 collagen. To avoid any effect of support glass plate on cellular mechano-sensing (Buxboim et al., 2010), we prepared thick gels (~400 µm), by keeping the volume of the gel solution constant at 200 µl. To induce G0 on soft PAA gels, cells were seeded at low density (1000 cells/cm^2) to avoid any cell-cell mechano-signaling via matrix (Reinhart-King et al., 2008) and cultured for 48 h in growth medium. Before seeding cells, excess collagen was removed and the gel was equilibrated in growth medium for 1 h. For reactivation studies, G0-arrested BMSC were harvested by trypsinization from the gel, and replated on tissue culture plastic in growth medium or lysed directly for RNA and protein isolation.

2.2. Immunofluorescent staining

Ki67 staining: Cells were fixed in 4% buffered formalin and were incubated overnight with Ki67 (Dako, 1:100) at 4 °C. After, cells were washed and incubated with a fluorescent secondary (Alexa Fluor, Life Technologies, 1:1000) for 1 h at RT, before counterstaining with DAPI (Sigma).

Actin & vimentin staining: hBMSC were fixed with 4% paraformaldehyde (PFA), pH 7 in 1% Triton-X-100 (Sigma) (1:1) for 1 min on ice. Cells were then washed twice with cytoskeleton stabilizing buffer (CSB) (60 mM PIPES (piperazine-*N*,*N*′-bis(2-ethanesulfonic acid)), 27 mM HEPES ((4-(2-hydroxyethyl)-1-piperazineethanesulfonic acid)), 10 mM EGTA ((ethylene glycol-bis(β-aminoethyl ether)-N,N,N′,N′-tetraacetic acid)), 4 mM magnesium sulphate (heptahydrate), pH 7), and fixed again with 4% PFA for 5 mins on ice. Cells were washed with CSB, blocked with 1.5% BSA in 0.5% Triton X-100 for 30 mins on ice and incubated with anti-vinculin antibody (Sigma, 1:400) overnight at 4 °C, detected with Alexa Fluor-568 Rabbit anti-mouse antibody (Thermo, 1:1000). Actin was detected with Alexa Fluor-488 Phalloidin (Thermo, 1:400) and nuclei counterstained with Hoechst 33342, prior to imaging on a laser scanning confocal microscope (LSM, Carl Zeiss).

BrdU staining: Cells were pulsed with 100 µM BrdU (Sigma) for 1 h at 37 °C, then processed for detection of incorporated BrdU using anti-BrdU antibody (DSHB, 1:100) as described (Dhawan and Helfman, 2004).

2.3. RNA isolation and qPCR

Cells were lysed in 1 ml of TRIzol (Invitrogen) and total RNA was isolated per the manufacturer's recommendations and as previously published (Cheedipudi et al., 2015). RNA was quantified on nanodrop spectrophotometer (Thermo Scientific), and cDNA prepared with 1 µg of total RNA using Invitrogen SSIII RT kit as per manufacturer's protocol. Real time PCR was performed on ABI HT7000 and fold change was calculated by $2^{-\Delta\Delta Ct}$ method, using GAPDH to normalize values. List of primers used is provided in Supplementary Table 2.

2.4. CFU-assay

Pre-G0 or G0 (MC culture) cells were used for CFU-f assay as previously described (Subramaniam et al., 2013). hBMSC (500 cells) or

mBMSC (2000 cells) were plated in 100 mm dishes in growth medium, with medium replacement every third day. After 10 days, media was removed; the dish washed with PBS and colonies stained with 2% methylene blue (Sigma) solution (prepared in absolute ethanol) for 15 min at room temperature. Dishes were washed under running water to remove residual stain. Colonies were counted manually using stereomicroscope.

2.5. Osteoblast and adipocyte differentiation

G0 (MC culture) cells were reactivated in growth medium for 24 h (R24) before inducing differentiation. Osteoblast (OB) differentiation was performed on cells plated at a density of 20,000/cm^2. Osteogenic induction media contained MEM supplemented with 10% FBS, 10 mM β-glycerophosphate (Sigma), 50 μg/ml L-ascorbic acid-2-phosphate (Sigma), 10 nM dexamethasone (Sigma) and 10 nM 1,25 hydroxy-vitamin D3 (Sigma) for 21 days, media were changed every 3 days. Adipogenesis (AD) was induced on cells plated at 30,000/cm^2 in media containing 10% FBS, 10% horse serum, 450 μM 1-methyl-3-isobutylxanthine (IBMX, Sigma), 5 μg/ml insulin (Sigma) and 1 μM rosiglitazone (Cayman Chemical) for 15 days, media was replaced every 3 days. Alkaline phosphatase activity was measured as previously published (Harkness et al., 2016).

2.6. Cytochemical staining

Staining was performed on cells undergoing osteogenic and adipogenic differentiation. Briefly, osteogenesis was detected by fixing cells in ice cold 70% EtOH for 1 h at −20 °C, incubating in 40 mM alizarin red dye (pH 4.2) (AZR, Sigma), for 10 mins at RT, washed in water and PBS to remove excess stain. For quantification, AZR was eluted using 10% cetylpyridinium chloride (Sigma) and absorbance measured at 570 nm. Cells undergoing adipogenic differentiation were fixed in 4% formalin for 5 mins at RT, washed in 3% isopropanol and incubated with 0.5% oil red O (ORO, Sigma) in 60% isopropanol for 1 h at RT. Excess stain was removed by washing in water, ORO was eluted in absolute isopropanol and quantified at 510 nm on a FLUOstar Omega plate reader (BMG Labtech).

2.7. In vivo bone formation assay

Either pre-G0 or R24 hBMSC-TERT cells were used to perform heterotopic bone formation assay according to protocol described previously (Abdallah et al., 2008). Briefly, 500,000 cells (pre-G0 or R24) were mixed with hydroxy-apatite/tricalcium phosphate ceramic powder (HA/TCP, 40 mg; Zimmer Scandinavia) and incubated overnight at 37 °C in humidifying incubator. After, excess medium was removed and HA/TCP with hBMSC-TERT cells was transplantation on either side of the dorsolateral area of NOD/SCID mice. After 8 weeks, implants were harvested and fixed in 4% formaldehyde for 24 h, decalcified in formic acid for 3 days, and embedded in paraffin and sectioned. Sections were and stained with haematoxylin & eosin. Bone volume per total volume was blindly quantified using pixel scoring method as described previously (Abdallah et al., 2008). Human-specific vimentin staining (Thermo Scientific) was used to show that the cells in the implants were of human origin.

2.8. RNA/DNA staining

Cells were incubated with 10 μm Hoechst 33,342 (Sigma) for 45 mins at 37 °C. Cell pellets were then washed in PBS before incubation with 5 μM Pyronin Y (Sigma) with 0.1 μm Verapamil (Sigma; to inhibit dye efflux) for 30–45 min at 37 °C. Stained cells were collected on glass slides using a cytospin and imaged.

2.9. Microarray analysis

RNA was isolated from pre-G0, G0 (MC culture) and 24 h reactivated post-G0 (R24) hBMSC-TERT. Microarray processing was done at Genotypic Inc. Bangalore, India, using Agilent 60 K human whole genome gene expression arrays (one-colour array, experimental protocols are available on http://www.agilent.com). The data was extracted using Agilent Feature extraction software and analyzed using GeneSpring GX version 11.5 and normalized using the 75th percentile shift. Samples were compared as G0 vs Pre-G0, R24 vs G0 and R24 vs Pre-G0. Genes 2-fold up- and down-regulated in test samples with respect to controls were identified (Supplementary Table 3). Differentially regulated genes during G0 and R24 were used to generate PCA plot (ClustVis) and heatmap (Morpheus). Data was analyzed using online tool DAVID (Huang da et al., 2009). MIAME-compliant microarray data is deposited in NCBI GEO (Accession # GSE60608).

2.10. Statistical tests

Data is represented as the mean ± SEM and derived from at least three independent experiments. Graphs were produced using Microsoft Excel or Graphpad Prism software and statistically analyzed using Student's *t*-test.

3. Results

3.1. Modulation of cell adhesion induces BMSC to enter G0

In vitro, G0 or reversible cell cycle arrest is triggered by mitogen depletion (Pardee, 1974; Sage et al., 2000), anchorage deprivation (Macpherson and Montagnier, 1964, Benecke et al., 1978, Ben-Ze'ev et al., 1980), inhibition of cytoskeletal signaling (Dhawan and Helfman, 2004) or growth to confluence (Abercrombie, 1970). To generate G0 cultured BMSC, we modified protocols for suspension culture (Milasincic et al., 1996; Sellathurai et al., 2013) and culture on soft substrates (Winer et al., 2009) that have previously been described for inducing G0 in ASC. In suspension culture, BMSC were anchorage deprived in a viscous medium containing 1.3% MC whereas on soft PAA gels (0.6 kilopascal (kPa) stiffness) the cells were loosely attached and unable to exert sufficient contractile force to spread (Fig. 1A). We tested the proliferative behavior of hBMSC on PAA gels of varying stiffness and identified lower stiffness gels (≤1 kPa) were efficient in inhibiting hBMSC proliferation as determined by bromodeoxyuridine (BrdU) incorporation (Fig. S1A). In addition, compared to hBMSC cultured on stiff PAA gels (40 kPa) that formed robust actin stress fibers and focal adhesions, hBMSC cultured on soft PAA gels (0.6 kPa) failed to form stress fibers and focal adhesions (Fig. S1B).

We tested the functional properties of BMSC derived from three different sources-primary human BMSC (hBMSC), primary mouse BMSC (mBMSC) and a human telomerized BMSC cell line (hBMSC-TERT) (Simonsen et al., 2002). We observed a significant reduction in the percentage of ki67-positive cells (indicative of cycling cells) when primary hBMSC were cultured in MC suspension (> 5-fold, $p < 0.05$) or on soft PAA gels (> 3-fold, $p < 0.05$) (Fig. 1B). Similar results were obtained when hBMSC-TERT were cultured in MC suspension, (> 5-fold reduction in ki67 positive cells, $p < 0.05$) (Fig. S2A). Time course analysis revealed a rapid decline in the number of proliferating cells as early as 12 h following culture of hBMSC in MC suspension (Fig. 2A) and on soft PAA gels (Fig. 2B) and minimal DNA synthesis was observed after 48 h (Fig. 2A,B). Similar results were obtained with hBMSC-TERT (Fig. S2B) and mBMSC (Fig. S3A).

To determine whether cell cycle arrest induced by MC and soft PAA culture is reversible, BrdU incorporation was assessed after replating G0 arrested BMSC onto tissue culture plastic dishes. Replating of either MC suspension- or soft PAA gel-cultured BMSC on plastic tissue culture plastic dishes in growth medium (with 10% serum) led to synchronous

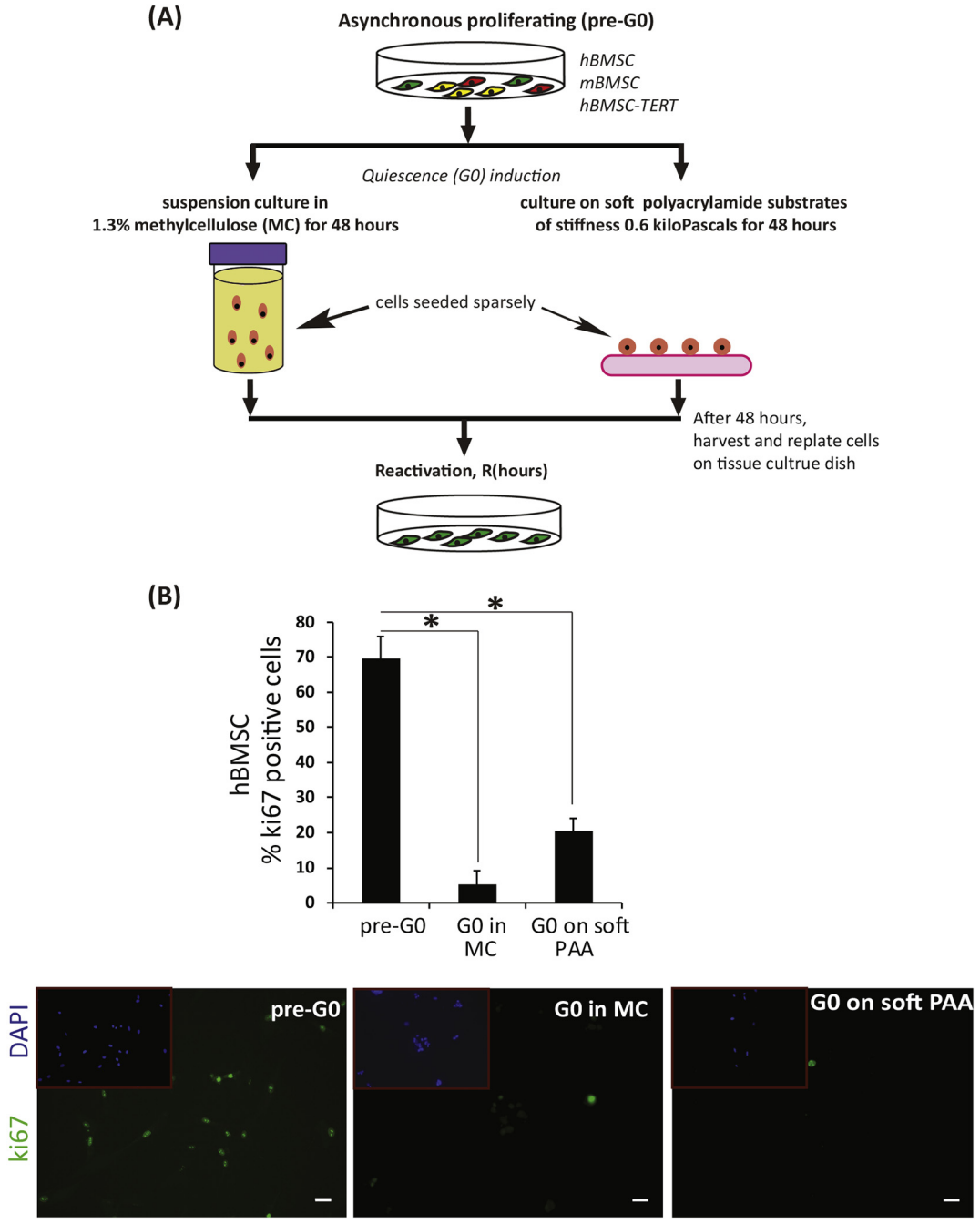

Fig. 1. G0 induction in BMSC.
(A) Methods to induce G0 in BMSC.
BMSC are maintained as asynchronous proliferating population (pre-G0) on tissue culture plastic dishes in growth medium. To induce G0 arrest, BMSC were cultured for 48 h in suspension medium composed of 1.3% methylcellulose (MC culture) or cultured on soft polyacrylamide (PAA) gels (0.6 kPa). For reactivation, G0 arrested cells were harvested and replated on tissue culture plastic dishes in growth medium.
(B) ki67 expression in pre-G0 and G0 arrested hBMSC.
Assessment of ki67 expression in hBMSC during pre-G0, G0 in MC and G0 on 0.6 kPa PAA gel; ki67 in green; DAPI in blue, *$p < 0.05$, scale bar = 100 μm.

cell cycle re-entry as evidenced by increased BrdU incorporation beginning at 12 h of replating, with the number of labeled cells peaking between 24 and 36 h (> 10-fold increase compared to G0 (48 h), $p < 0.05$) (Fig. 2A,B). A similar trend was observed in hBMSC-TERT (Fig. S2B) and mBMSC (Fig. S3A). These experiments demonstrate that both human and mouse primary BMSC attain a reversible G0 state when cultured in suspension or on soft gels.

3.2. Regulation of cell cycle genes during G0 entry and exit

We analyzed the expression of positive and negative regulators of cell cycle in hBMSC during G0. Cyclin D1 (CCND1), an important regulator of G1-S transition was down regulated in G0 arrested hBMSC (> 2-fold, $p < 0.05$) (Fig. 3A). Similarly, the expression of cyclin A2 (CCNA2), cyclin B1 (CCNB1) and cyclin E1 (CCNE1) were down regulated significantly ($p < 0.05$) in G0 hBMSC (Fig. 3A). The marked increase in CCNA2 and CCNE1 in 24 h reactivated (R24) cells compared

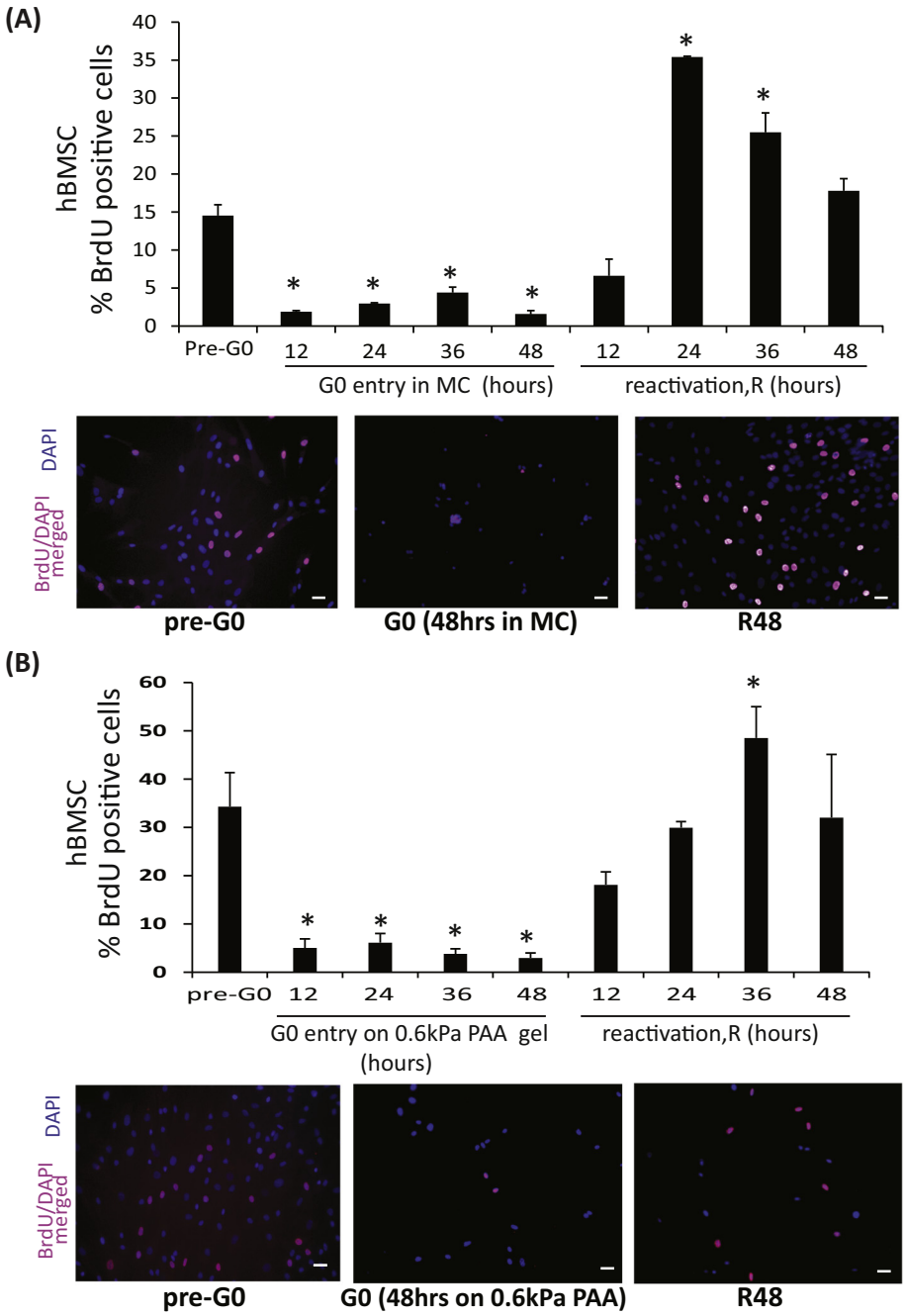

Fig. 2. Kinetics of G0 entry and reactivation in hBMSC.
(A) Detection of BrdU incorporation in primary hBMSC during pre-G0, G0 entry in MC and reactivation, R (hours) (B) Detection of BrdU incorporation in primary hBMSC during pre-G0, G0 entry on 0.6 kPa PAA gel and reactivation, R (hours); BrdU-DAPI merged in magenta, DAPI in blue, *$p < 0.05$, scale bar = 100 μm.

to pre-G0 cells reflects the synchronous nature of the population following a period in G0 (Fig. 3A). In addition, negative regulator of cell cycle cyclin dependent kinase inhibitor (CKI)-p21 and p27 was strongly up-regulated in G0 hBMSC (> 2-fold, $p < 0.05$) (Fig. 3A). During reactivation (R24), the expression of the cyclins and CKI were restored (> 2-fold change in expression, $p < 0.05$), confirming the reversibility of G0-associated changes in cell cycle gene program (Fig. 3A). Similar results were obtained with hBMSC-TERT (Fig. S2C) and mBMSC (Fig. S3B).

To examine whether induction of G0 in hBMSC affects their self-renewal, we determined colony-forming capacity before and after induction of G0. G0 BMSC exhibited a significantly increased number of colony-forming unit-fibroblast (CFU-f) compared to pre-G0 BMSC ($p < 0.05$) (Figs. 3B, S3C).

Previous studies have reported that G0 in mammalian cells is associated with reversible suppression of RNA synthesis (Ben-Ze'ev et al., 1980). To visualize RNA content in MC-cultured BMSC, we stained cells with Pyronin-Y. As shown in Fig. S2D, global RNA content of G0 hBMSC-TERT was significantly decreased as compared to pre-G0 cells and restored during post-G0 reactivation (R24).

3.3. Differentiation capacity of BMSC following post-G0 reactivation

To address whether induction of G0 affect differentiation capacity of BMSC, we assessed adipocytic (AD) and osteoblastic differentiation (OB) potential of pre-G0 and post-G0 reactivated (R24) hBMSC-TERT.

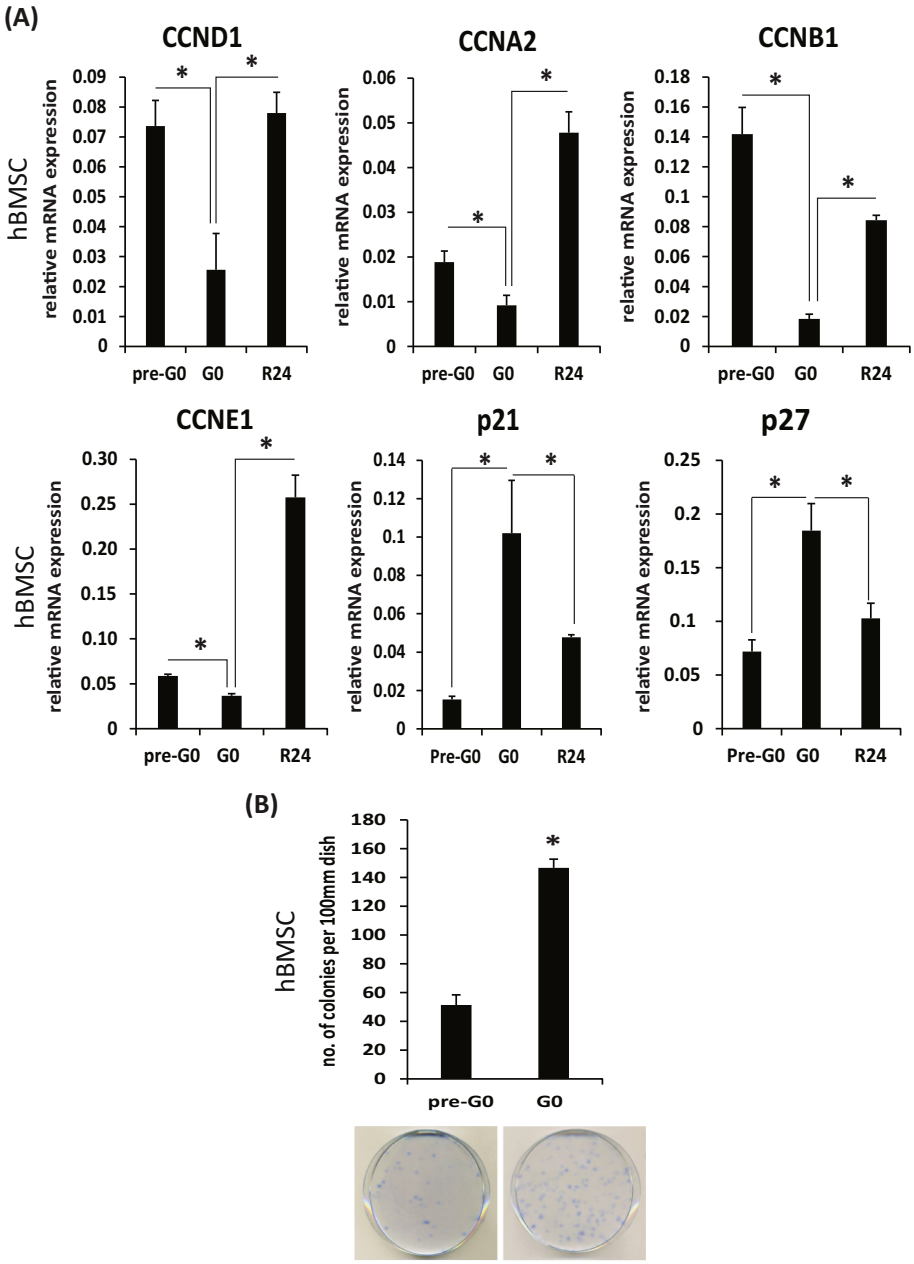

Fig. 3. G0 entry and exit in hBMSC.
(A) Detection of levels of cyclins (CCNA2, CCNB1, CCND1, CCNE1) & CKIs (p21 & p27) during pre-G0, G0 (MC culture) and R24 (reactivation 24 h) by qRT-PCR (B) analysis of self-renewal in pre-G0 and G0 (MC culture) in hBMSC by CFU-f, *$p < 0.05$.

We observed significantly increased gene expression levels of osteoblastic genes-osteopontin (OPN), RUNX2, and alkaline phosphatase (ALP) (OB day 7) (Fig. 4A), increased ALP activity (OB day 7) (Fig. 4B) and increased mineralized matrix formation (OB day 14) (Fig. 4C) in R24 reactivated cells. To determine whether the in vitro enhanced osteoblast differentiation ability of reactivated hBMSC-TERT coincides with bone formation in vivo, we tested the ectopic bone formation ability of R24 cells. Indeed, R24 hBMSC-TERT cells display an increased ability to form bone in an ectopic model of bone formation ($n = 4$, $p < 0.05$) (Fig. 4D). By contrast, adipocyte differentiation was compromised, as upon AD induction, R24 hBMSC-TERT exhibited lower adipocyte differentiation capacity, evidenced by lower gene expression levels of PPARγ, adiponectin (adipoQ) and adipocyte protein-2 (aP2) (AD day 7) (Fig. 4E) and less oil droplets accumulation (AD day 14) (Fig. 4F).

3.4. Global gene expression profile of G0 and reactivated hBMSC

To explore global changes in gene expression associated with induction of G0 and post-G0 reactivation (R), we performed gene expression profiling of hBMSC-TERT in the following conditions: pre-G0 (asynchronously proliferating), G0 (cell cycle arrested following 48 h in MC) and 24 h reactivated post-G0 (R24). Principle component analysis (PCA) demonstrated clear clustering of sample replicates at each time point demonstrating reproducibility of the data and induction of a specific genetic program (Fig. 5A).

To visualize co-regulated genes during G0 and reactivation, we generated a heatmap of differentially regulated genes in three conditions (pre-G, G0 & R24) that revealed two categories of co-regulated genes (1) genes suppressed during G0 and (2) genes induced in G0 (Fig. 5B). In addition, heatmap showed that changes in gene expression

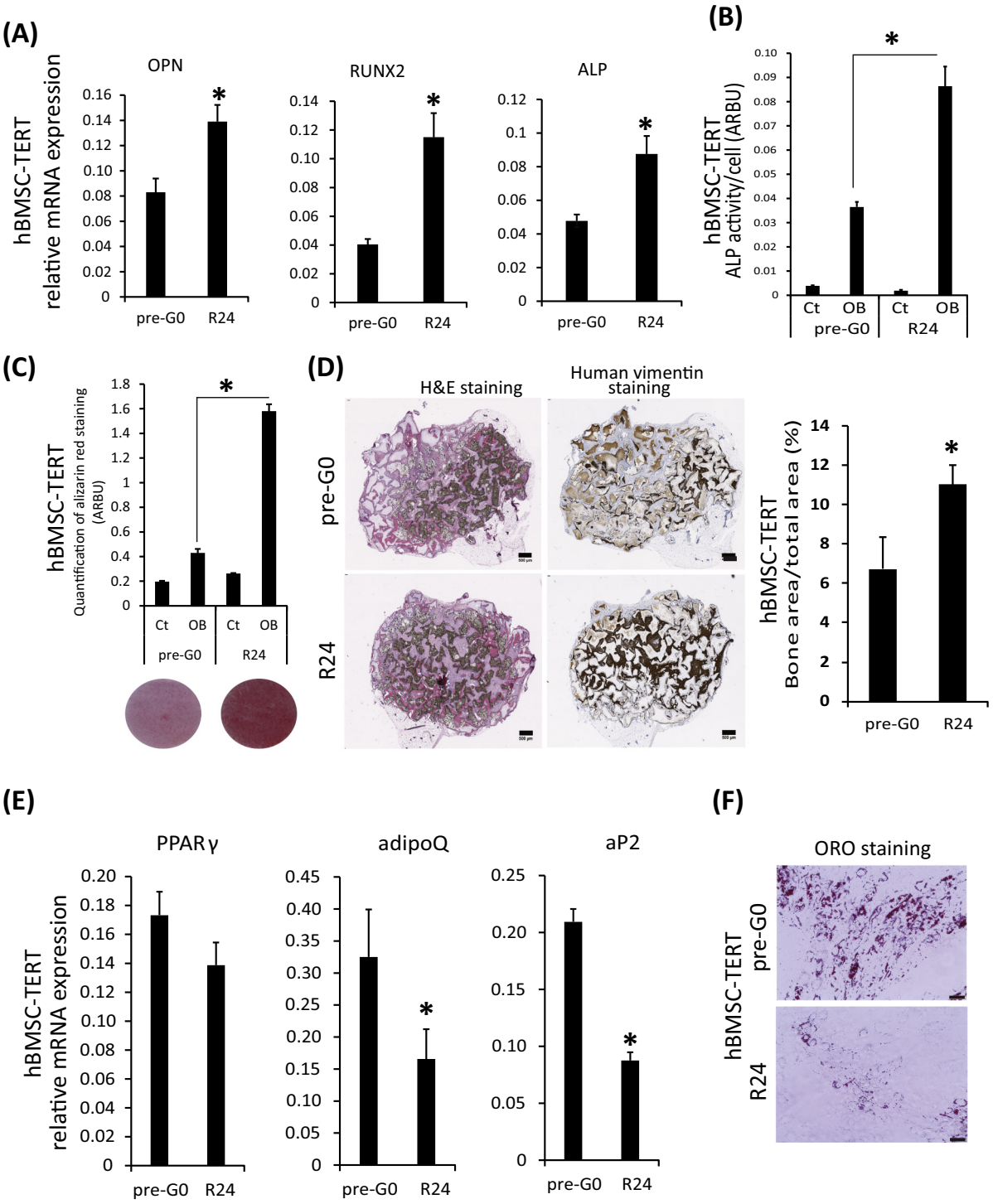

Fig. 4. Assessment of differentiation potential of pre-G0 and reactivated (R24) hBMSC-TERT.
(A) Detection of mRNA levels of osteopontin (OPN), Runx2 and alkaline phosphatase (ALP) at day 7 of OB induction by qPCR, (B) detection of ALP activity at day 7 of OB induction, (C) alizarin red staining and quantification at day 14 of OB induction, (D) quantification of in vivo ectopic bone formation in NOD-SCID mice after 8 weeks of implantation (scale bar = 500 μm), (E) detection of mRNA levels of PPARγ, adipocyte protein-2 (ap2) and adiponectin (adipoQ) at day 7 of AD induction by qPCR, (F) oil red O staining at day 14 of AD induction (scale bar = 100 μm), *$p < 0.05$.

induced during G0 are not completely reversible within 24 h of re-activation (R24), suggesting that the molecular changes during G0 exert long-term effects on cellular phenotype. During G0, 5069 genes were differentially regulated (> 2-fold up or down regulated) as compared to pre-G0 cells (Fig. 5C). At 24-h reactivation (R24), we observed 5084 genes differentially regulated (> 2-fold up or down regulated) as compared to G0 cells (Fig. 5C). Interestingly, comparing molecular signature of reactivated sample R24 with pre-G0 proliferating cells, revealed significant differences with 4443 genes (> 2-fold up or down regulated) differentially regulated (Fig. 5C), consistent with retention of population synchrony following cell cycle re-entry.

To classify the differentially expressed genes during G0, we performed gene ontology (GO) analysis using online tool DAVID. As expected, genes down-regulated in G0 were enriched in several categories

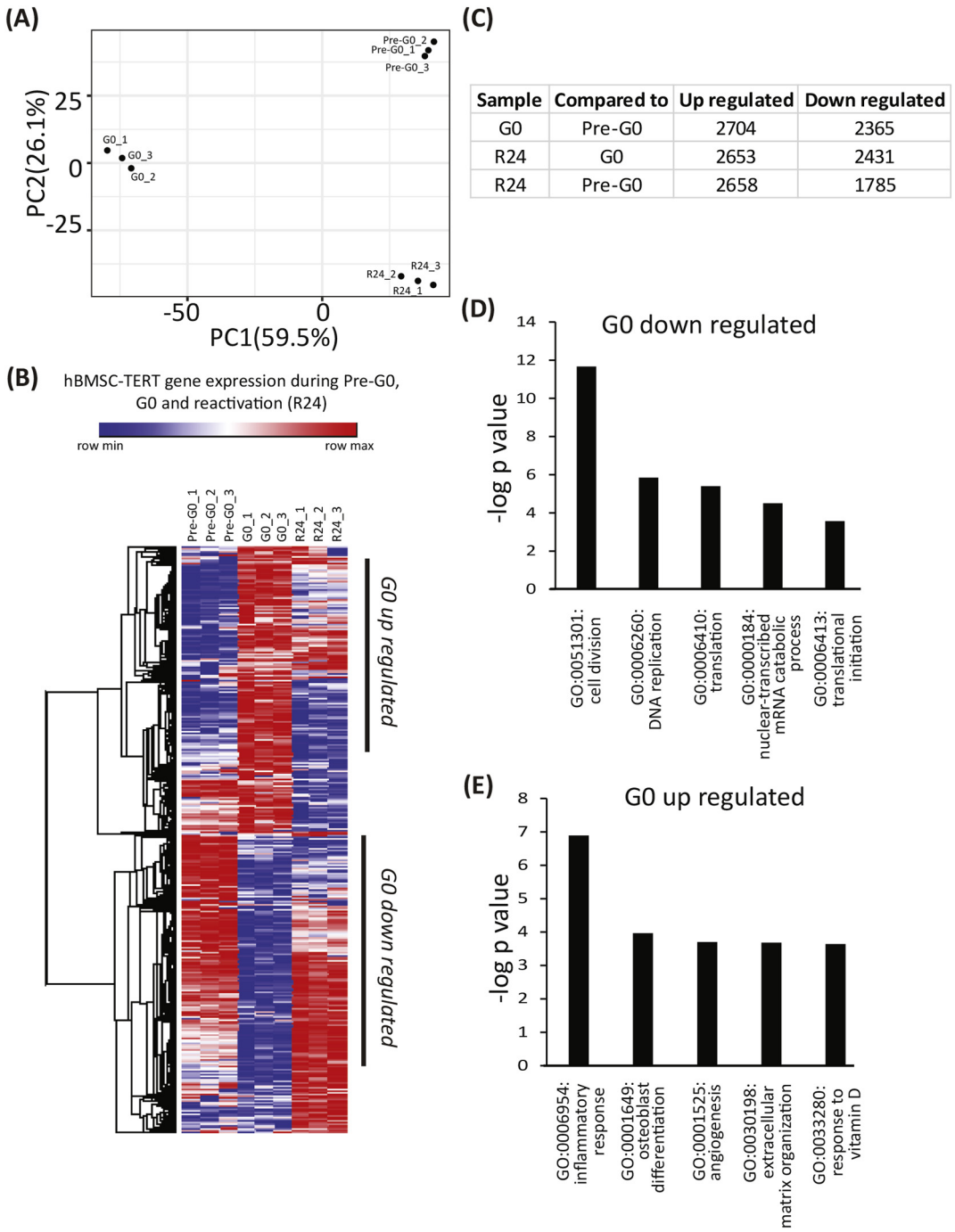

Sample	Compared to	Up regulated	Down regulated
G0	Pre-G0	2704	2365
R24	G0	2653	2431
R24	Pre-G0	2658	1785

Fig. 5. Gene expression profiling of pre-G0, G0 (MC culture) and reactivated (R24) hBMSC-TERT using microarrays.
(A) PCA plot depicting transcriptome of samples used in the study (pre-G0, G0 & R24), (B) heat map depicting co-regulated genes in G0 and R24, (C) number of differentially regulated genes (> 2-fold), (D&E) gene ontology (GO) term enriched in significant down regulated and up regulated genes during G0.

related to *cell division* (KIFC1, CCNE2, CDC42, CCNA2, CDC6, FBXO5, CCNB1, CCNB2) and *DNA replication* (CLSPN, DBF4, TIPIN, POLA2). In muscle stem cells, it has been shown that G0 state is associated with suppressed protein synthesis (Zismanov et al., 2016). Interestingly, we also observed down regulation of genes regulating *translation/translation initiation* (MRPS36, RPL17, RPL36A, MRPS33, MRPS14, ABCE1, RPL17, RPL36A) suggesting global suppression of translation in G0 hBMSC-TERT. Suppression of genes regulating *nuclear-transcribed mRNA catabolic process* (RPL17, RPL36A, RPL35, RPS15A, RPL23A) suggest an increase mRNA turnover in G0 hBMSC-TERT cells (Fig. 5D).

Genes upregulated in G0 hBMSC-TERT cells suggest an enhanced osteogenic potential of these cells as they were enriched for ontology (GO) terms including *osteoblast differentiation* (IBSP, BMP2, ITGA11, WNT11, SPP1, BMP6, TWIST1), *extracellular matrix organization* (ITGA10, ITGB3, LAMB3, ITGAX, COL7A1) and *response to vitamin D* (STC2, PTGS2, STC1, CD4, BMP7, SPP1). Further, upregulation of genes regulating *angiogenesis* (SAT1, FGF18, VEGFA, PECAM1, HIF3A) and *inflammatory response* (PTSG2, IL10, IL1A. IL1B, CCR7) in G0 hBMSC-TERT cells suggest a distinct paracrine activity of these cells (Fig. 5E). Relevant pathways enriched in G0 hBMSC-TERT are depicted in Fig. 6A, important pathways include *metabolic pathways* (AUH, AMY1C, IMPA2, GAA, TK2, PTGS1), *regulation of actin-cytoskeleton* (PXN, ITGB3, ITGAX, PIK3R2, ITGA11, ITGA10), *TGF-beta signaling pathway* (BMP8B, BMP2, SMAD7, BMP7, BMP6, ID2, ID1, ID4, ID3, THBS2) and *Wnt-*

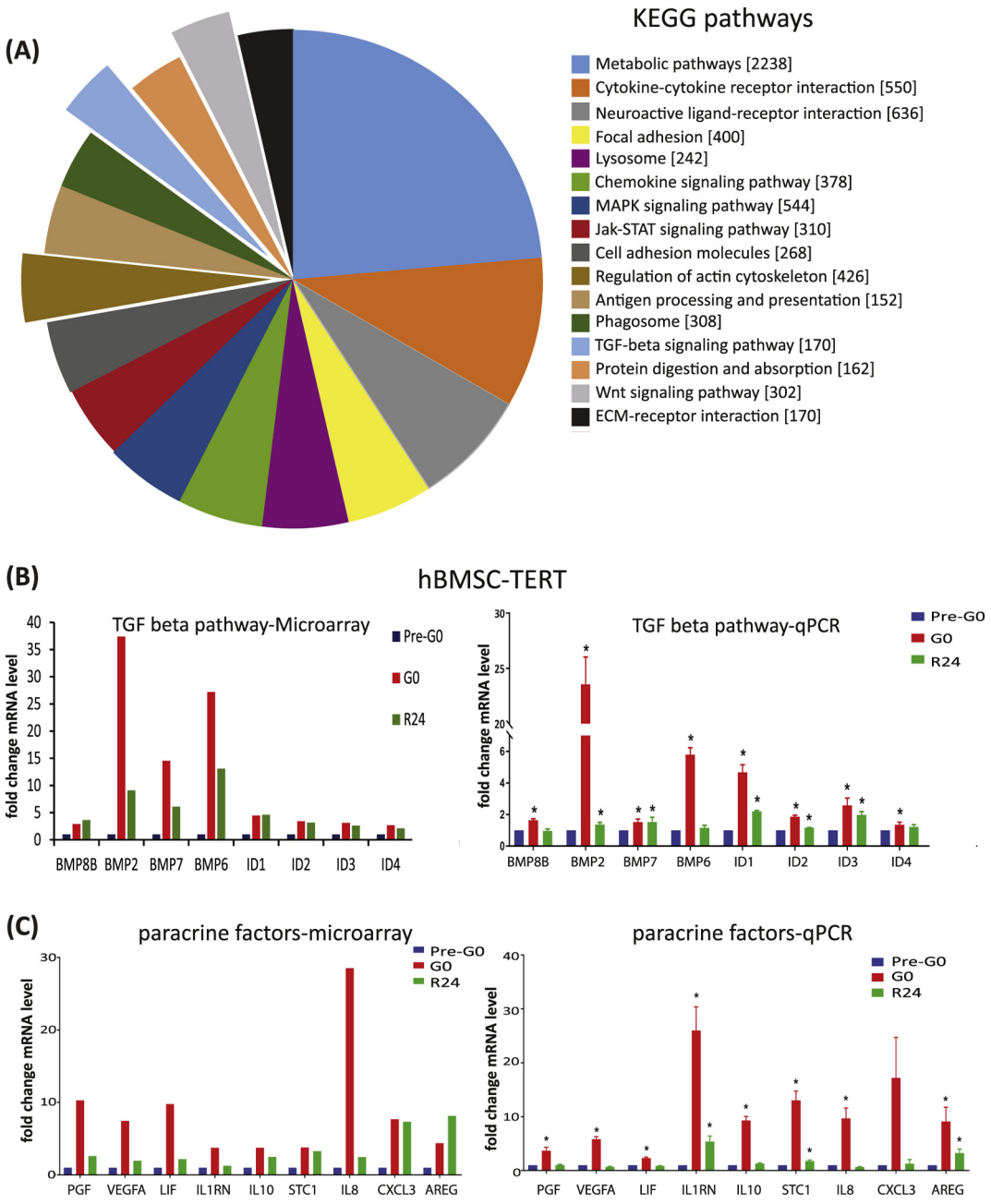

Fig. 6. Pathways and paracrine factors in G0 (MC culture) hBMSC-TERT.
(A) Pie chart representing fraction of genes of particular pathways enriched in G0 hBMSC-TERT, (B) representative genes enriched in TGF beta/BMP signaling pathway in microarray & validated by qPCR, (C) expression of paracrine factors-PGF, VEGFA, LIF, IL1RN, IL10, STC1, IL8, CXCL3, and AREG in pre-G0, G0 and R24 hBMSC-TERT in microarray & validated by qPCR.

signaling pathway (AXIN2, WNT7B, FZD8, WNT5A, WNT11,). Due to their relevance to hBMSC biology, we chose several BMP signaling genes that were upregulated during G0 to validate by qRT-PCR. As seen in Fig. 6B there was a good correlation between microarray results and qRT-PCR.

3.5. Effect of G0 on hBMSC paracrine factors expression

Clinical transplantation of BMSC has been employed to enhance tissue regeneration in a number of clinical conditions, as they secrete a large number of bio-active molecules with possible anti-inflammatory, tissue protective or regenerative effects (Vizoso et al., 2017). To determine the profile of therapeutically relevant secreted factors, we mined the microarray data to reveal the effects of reversible G0 on gene expression of BMSC secreted factors. Several known MSC derived paracrine factors were significantly up-regulated during G0 (> 2-fold) including interleukin receptor 1 antagonist (IL1RN) (Ortiz et al., 2007), stanniocalcin 1 (STC1) (Bartosh et al., 2010), interleukin 10 (IL10) (Choi et al., 2008), placental growth factor (PGF) (Marrony et al., 2003), vascular endothelial growth factor A (VEGFA) (Matsumoto et al., 2005), leukemia inhibitory factor (LIF) (Nasef et al., 2008), interleukin 8 (IL8) (Kim et al., 2009), c-x-c motif chemokine ligand 3 (CXCL3) (Lee et al., 2012) and amphiregulin (AREG) (Kerpedjieva et al., 2012) and these changes were validated using qRT-PCR (Fig. 6C).

4. Discussion

Several studies have suggested that a subpopulation of BMSC are in

G0 state within the in vivo niche (Peiffer et al., 2007; Morikawa et al., 2009); however, an explicit analysis of G0 biology has not been reported. Here, we report a detailed cellular and molecular phenotypic characterization of the G0 state in hBMSC. First, we report two simple and efficient methods for generating homogeneous populations of G0 BMSC based on changing cellular adhesive properties through culturing in viscous medium or on soft substrates. Second, we extensively characterize this cellular state. Finally, we demonstrate that by passage through a G0 state, BMSC acquire enhanced potential for clonogenic self-renewal (CFU-f) and osteoblastic differentiation, both in vitro and in vivo.

Cultured mammalian cells can be induced to enter G0 state by manipulating variables that are necessary for active proliferation such as contact inhibition (Macpherson and Montagnier, 1964, Philips et al., 1999) or mitogen-deprivation (Gustincich and Schneider, 1993). However, previous studies have reported that contact inhibition is inefficient in suppressing hBMSC proliferation (Oskowitz et al., 2011) and that mitogen-deprivation induces early replicative senescence (Ho et al., 2011). Alternatively, modulating adhesion-dependent signaling pathways either by complete deprivation of cell anchorage using suspension culture in methylcellulose (MC) (Milasincic et al., 1996) or by direct inhibition of actomyosin contractility using small molecule inhibitors (Dhawan and Helfman, 2004) have been used to induce G0, even in mitogen-rich media. We observed that both suspension culture in MC or plating on soft PAA substrates were efficient in inducing G0 state in BMSC. For G0 induction, MC culture is advantageous over PAA as preparation of the viscous medium is simple and large number of homogenous quiescent cells can be generated in relatively less volume (one million cells per 10 ml of MC suspension). One of the major disadvantage of MC culture is that it is not possible to replenish the culture medium therefore cell cannot survive once the nutrients are exhausted.

We observed that induction of G0 in BMSC led to significant changes in cellular and molecular phenotype. This corroborates our previous findings in other cultured cell types (Sellathurai et al., 2013; Subramaniam et al., 2013). The G0 state has been shown in freshly isolated HSC and muscle stem cells to promote tolerance of proliferation-associated genetic stresses, protection from cytotoxic agents and preservation of genome integrity, due to low probability of incorporating deleterious mutations (Pallafacchina et al., 2010; Mourikis et al., 2012). The biological importance of G0 state can also be gauged from reports that associate loss of quiescence with accelerated aging (Sousa-Victor et al., 2014, Mendelsohn and Larrick, 2016) and pathological cellular changes (Cheung and Rando, 2013).

Induction of G0 in BMSC led to decreased DNA synthesis, repressed global RNA levels, decreased expression of cyclins, and increased expression of CKI. These data are similar to the reported characteristics of G0 mouse fibroblasts and human myoblasts (Sellathurai et al., 2013; Subramaniam et al., 2013) and demonstrate the universal nature the G0 phenotype. Interestingly, similar to primary hBMSC, the immortalized hBMSC-TERT cell line (Simonsen et al., 2002), despite expression of high level of telomerase activity responded to anchorage deprivation suggesting retention of tumor suppressive mechanisms of anchorage-dependence.

Most studies examining the biology of BMSC employed asynchronized proliferating cultures that may not reflect critical aspects of the in vivo biology of these adult stem cells, our data provide some insight into these differences. For example, we found that the transcriptome of G0 hBMSC was markedly different from that of asynchronized proliferating (pre-G0) hBMSC and the genes reversibly suppressed during G0 were cell cycle regulators as has been reported in other cell types including myoblasts and fibroblasts (Sachidanandan et al., 2002). Differences in gene expression of pre-G0 and reactivated R24 cells were intriguing, even though both samples were adherent and cycling. It is well known that G0-synchronized cells exhibit extended kinetics of entry into S phase compared to asynchronously proliferating cells (Coller, 2007) and this observation supports the idea that the first cell cycle following G0 is distinct from subsequent cycles when exponential cell kinetics are restored. Also, previous studies have demonstrated that the first cell cycle following G0 is distinct from subsequent cycles as duration of G1 phase of first cell-cycle after G0 is considerably larger (Coller, 2007).

G0 is usually associated with reversible suppression of lineage-specific gene expression (Milasincic et al., 1996, Dhawan and Helfman, 2004), suggesting that this cellular state promotes self-renewal. We observed that induction of G0 in hBMSC led to shift in lineage fate choice with increased capacity for osteoblast differentiation and decreased adipocyte differentiation. It might be possible that MC culture select for pre-osteoblastic cells at the expense of pre-adipocytic cells (Post et al., 2008). However, we did not observe severe change in cell number or cell death following G0 culture, making this explanation improbable. It is also possible that induction of G0 may enhance epigenetic imprinting of the tissue of origin, which, for hBMSC is osteogenic. In support of this concept, we found enhanced expression of known positive modulators of TGFβ/BMP signaling pathway during G0 and R24. BMP signaling is important for osteoblast differentiation as demonstrated by several in vitro studies that reported that BMP-2, BMP-6 and BMP-7 enhance osteoblast differentiation of hBMSC (Peng et al., 2004; Sammons et al., 2004; Ho et al., 2016). Downstream effectors of BMP-signaling, the helix-loop-helix proteins-inhibitor of DNA binding/differentiation (Id), mediate BMP-induced osteoblast differentiation of BMSC (Peng et al., 2004). BMP9 stimulation of MSC enhances gene expression of Id1, Id2 and Id3 and induces osteoblastic differentiation (Peng et al., 2004). On the other hand, loss of Id proteins diminishes BMP9 induced osteogenic differentiation in MSC (Peng et al., 2004). In accordance, we found enhanced expression of Id1, Id2, Id3 and Id4 during G0 and in post-G0 reactivated (R24) hBMSC-TERT. Previous studies showed a role of Wnt-signaling in regulating G0 state in muscle stem cells (Sellathurai et al., 2013; Subramaniam et al., 2013). Our study supports these previous observations as components of Wnt-signaling were induced in G0 hBMSC-TERT.

The enhanced expression of transcripts encoding therapeutically relevant secreted factors including growth factors (VEGFA, PGF, LIF), anti-inflammatory (IL1RN, IL10, STC1) and chemokines (IL8, CXCL3, AREG) in G0 hBMSC-TERT cells suggests an altered secretome and important changes in paracrine signaling. BMSC-derived VEGFA is known to enhance neovascularization in animal model of myocardial infarction (Matsumoto et al., 2005), while BMSC-derived PGF might play a role in angiogenesis and hematopoiesis (Marrony et al., 2003). The anti-inflammatory role of BMSC-derived IL1RN and IL10 has been shown in animal model of lung injury and arthritis respectively (Ortiz et al., 2007; Choi et al., 2008).

Quiescent cells are reported to be highly metabolically active despite being non-dividing (Lemons et al., 2010) and exhibit increased glycolysis, which is a hallmark of self-renewal in stem cells (Shyh-Chang et al., 2013). Enrichment of metabolic pathways in our transcriptome analysis of G0 BMSC supports this observation and might explain increased self-renewal ability of the cells post-G0. In one previous study, Witkowska et al., have shown that osteoblastic differentiation of BMSC was enhanced when cultured on stiff compared to soft PAA substrates (Witkowska-Zimny et al., 2013). However, the soft PAA employed in that report was much stiffer (1.46 kPA) than the one used in our study (0.6 kPA), which was reflected as continued proliferation evidenced by increased cell number (Witkowska-Zimny et al., 2013). In our experiments, we also employed a low seeding density on soft PAA, which prevented cell-cell contact (Venugopal et al., 2018), and together resulted in induction of G0. Thus, the changes we report in BMSC biology were not dependent on external mechanical determinants of the PAA gel but on the induction of the G0 state by the altered contractility experienced by cells.

Our study does not address some important issues that are avenues for future investigation. Since the culture conditions in vitro do not reflect the in vivo environment, further studies are required to assess

how closely the molecular phenotype can be extrapolated to BMSC in vivo. Also, while we could show that BMSC reprogrammed into the G0 state in culture exhibit enhanced bone formation capacity in vivo, the therapeutic relevance of our findings need confirmation employing in vivo bone regeneration models. Further, using the current culture condition, we cannot exclude that part of the observed changes in the molecular phenotype of BMSC induced to enter G0 was caused by material cues irrespective of G0 state (Crowder et al., 2016). However, our earlier studies in myoblasts show that perturbation of either adhesion or mechanical cues converges on signaling pathways that lead a cell into quiescence (Dhawan and Helfman, 2004, Gopinath et al., 2007). Induction of G0 by different methods (contact inhibition, loss of adhesion and mitogen deprivation) is associated with a characteristic molecular phenotype irrespective of the material cues as demonstrated in fibroblasts (Coller et al., 2006) by transcriptional profiling. Finally, cell surface markers from our G0 transcriptome data could be used to validate or purify mononuclear cells from the bone marrow, and G0 BMSC could also be tested in animal models for their efficacy in disease models.

5. Conclusion

Methylcellulose culture and soft substrate culture methods are efficient to induce G0 state in BMSC. Induction of G0 state in BMSC enhances stemness-phenotype including clonogenic self-renewal and osteoblastic differentiation and in vivo ectopic bone formation. These findings are relevant for future studies addressing aspects of the in vivo biology of BMSC and may provide a simple method for improving "BMSC functional cell quality" needed for therapeutic BMSC trials in regenerative medicine.

Supplementary data to this article can be found online at https://doi.org/10.1016/j.scr.2018.05.010.

Conflict of interest

The authors declare no conflict of interest.

Acknowledgements

We gratefully acknowledge facilities at the Bangalore Life Sciences Cluster (Animal Facility and CIFF for imaging and flow cytometry at C-CAMP, inStem,/NCBS Bengaluru, India). We acknowledge Pankaj M. for imaging. We acknowledge Genotypic Technology Private Limited Bangalore for microarray processing.

Funding

This work was supported by an Indo-Danish Grant of the Danish Foundation (grant no. BT/IN/Denmark/02/PDN/2011) for Strategic Research and the Govt of India Dept of Biotechnology (JD, MK), funds from InStem and CCMB (JD), doctoral fellowship from CSIR (MR) and postdoctoral fellowship from DBT (MSP). AM acknowledges fellowship support from the Wellcome Trust-DBT India Alliance (Project# IA/E/11/1/500419) for this work. Animal work was partially supported by the National Mouse Research Resource (NaMoR) grant (BT/PR5981/MED/31/181/2012;2013-2016) from the DBT to NCBS. MK received funding from the Danish Innovation fund, IndoDanish collaborative program (5166-00002A) the NovoNordisk foundation (NNF15OC0016284) and the Lundbeck foundation (R266-2017-4250)

References

Abdallah, B.M., Ditzel, N., Kassem, M., 2008. Assessment of bone formation capacity using in vivo transplantation assays: procedure and tissue analysis. Methods Mol. Biol. 455, 89–100. http://dx.doi.org/10.1007/978-1-59745-104-8_6.

Abercrombie, M., 1970. Contact inhibition in tissue culture. In Vitro 6 (2), 128–142.

Arora, R., Rumman, M., Venugopal, N., Gala, H., Dhawan, J., 2017. Mimicking muscle stem cell quiescence in culture: methods for synchronization in reversible arrest. Methods Mol. Biol. 1556, 283–302. http://dx.doi.org/10.1007/978-1-4939-6771-1_15.

Bartosh, T.J., Ylostalo, J.H., Mohammadipoor, A., Bazhanov, N., Coble, K., Claypool, K., Lee, R.H., Choi, H., Prockop, D.J., 2010. Aggregation of human mesenchymal stromal cells (MSCs) into 3D spheroids enhances their antiinflammatory properties. Proc. Natl. Acad. Sci. U. S. A. 107 (31), 13724–13729. http://dx.doi.org/10.1073/pnas.1008117107.

Benecke, B.J., Ben-Ze'ev, A., Penman, S., 1978. The control of mRNA production, translation and turnover in suspended and reattached anchorage-dependent fibroblasts. Cell 14 (4), 931–939.

Ben-Ze'ev, A., Farmer, S.R., Penman, S., 1980. Protein synthesis requires cell-surface contact while nuclear events respond to cell shape in anchorage-dependent fibroblasts. Cell 21 (2), 365–372.

Bianco, P., Robey, P.G., 2015. Skeletal stem cells. Development 142 (6), 1023–1027. http://dx.doi.org/10.1242/dev.102210.

Buxboim, A., Ivanovska, I.L., Discher, D.E., 2010. Matrix elasticity, cytoskeletal forces and physics of the nucleus: how deeply do cells 'feel' outside and in? J. Cell Sci. 123 (Pt 3), 297–308. http://dx.doi.org/10.1242/jcs.041186.

Cai, M., Shen, R., Song, L., Lu, M., Wang, J., Zhao, S., Tang, Y., Meng, X., Li, Z., He, Z.X., 2016. Bone marrow mesenchymal stem cells (BM-MSCs) improve heart function in swine myocardial infarction model through paracrine effects. Sci. Rep. 6, 28250. http://dx.doi.org/10.1038/srep28250.

Cheedipudi, S., Puri, D., Saleh, A., Gala, H.P., Rumman, M., Pillai, M.S., Sreenivas, P., Arora, R., Sellathurai, J., Schroder, H.D., Mishra, R.K., Dhawan, J., 2015. A fine balance: epigenetic control of cellular quiescence by the tumor suppressor PRDM2/RIZ at a bivalent domain in the cyclin a gene. Nucleic Acids Res. 43 (13), 6236–6256. http://dx.doi.org/10.1093/nar/gkv567.

Cherry, H.M., Roelofs, A.J., Kurth, T.B., De Bari, C., 2014. In vivo phenotypic characterisation of nucleoside label-retaining cells in mouse periosteum. Eur. Cell Mater. 27, 185–195 discussion 195.

Cheung, T.H., Rando, T.A., 2013. Molecular regulation of stem cell quiescence. Nat. Rev. Mol. Cell Biol. 14 (6), 329–340. http://dx.doi.org/10.1038/nrm3591.

Choi, J.J., Yoo, S.A., Park, S.J., Kang, Y.J., Kim, W.U., Oh, I.H., Cho, C.S., 2008. Mesenchymal stem cells overexpressing interleukin-10 attenuate collagen-induced arthritis in mice. Clin. Exp. Immunol. 153 (2), 269–276. http://dx.doi.org/10.1111/j.1365-2249.2008.03683.x.

Coller, H.A., 2007. What's taking so long? S-phase entry from quiescence versus proliferation. Nat. Rev. Mol. Cell Biol. 8 (8), 667–670. http://dx.doi.org/10.1038/nrm2223.

Coller, H.A., Sang, L., Roberts, J.M., 2006. A new description of cellular quiescence. PLoS Biol. 4 (3), e83. http://dx.doi.org/10.1371/journal.pbio.0040083.

Crowder, S.W., Leonardo, V., Whittaker, T., Papathanasiou, P., Stevens, M.M., 2016. Material cues as potent regulators of epigenetics and stem cell function. Cell Stem Cell 18 (1), 39–52. http://dx.doi.org/10.1016/j.stem.2015.12.012.

Dhawan, J., Helfman, D.M., 2004. Modulation of acto-myosin contractility in skeletal muscle myoblasts uncouples growth arrest from differentiation. J. Cell Sci. 117 (Pt 17), 3735–3748. http://dx.doi.org/10.1242/jcs.01197.

Gopinath, S.D., Narumiya, S., Dhawan, J., 2007. The RhoA effector mDiaphanous regulates MyoD expression and cell cycle progression via SRF-dependent and SRF-independent pathways. J. Cell Sci. 120 (Pt 17), 3086–3098. http://dx.doi.org/10.1242/jcs.006619.

Granero-Molto, F., Weis, J.A., Miga, M.I., Landis, B., Myers, T.J., O'Rear, L., Longobardi, L., Jansen, E.D., Mortlock, D.P., Spagnoli, A., 2009. Regenerative effects of transplanted mesenchymal stem cells in fracture healing. Stem Cells 27 (8), 1887–1898. http://dx.doi.org/10.1002/stem.103.

Gustincich, S., Schneider, C., 1993. Serum deprivation response gene is induced by serum starvation but not by contact inhibition. Cell Growth Differ. 4 (9), 753–760.

Haas, R.J., Bohne, F., Fliedner, T.M., 1969. On the development of slowly-turning-over cell types in neonatal rat bone marrow (studies utilizing the complete tritiated thymidine labelling method complemented by C-14 thymidine administration). Blood 34 (6), 791–805.

Harkness, L., Zaher, W., Ditzel, N., Isa, A., Kassem, M., 2016. CD146/MCAM defines functionality of human bone marrow stromal stem cell populations. Stem Cell Res Ther 7, 4. http://dx.doi.org/10.1186/s13287-015-0266-z.

Ho, J.H., Chen, Y.F., Ma, W.H., Tseng, T.C., Chen, M.H., Lee, O.K., 2011. Cell contact accelerates replicative senescence of human mesenchymal stem cells independent of telomere shortening and p53 activation: roles of Ras and oxidative stress. Cell Transplant. 20 (8), 1209–1220. http://dx.doi.org/10.3727/096368910X546562.

Ho, S.S., Vollmer, N.L., Refaat, M.I., Jeon, O., Alsberg, E., Lee, M.A., Leach, J.K., 2016. Bone morphogenetic Protein-2 promotes human mesenchymal stem cell survival and resultant bone formation when entrapped in Photocrosslinked alginate hydrogels. Adv. Healthc. Mater. 5 (19), 2501–2509. http://dx.doi.org/10.1002/adhm.201600461.

Huang da, W., Sherman, B.T., Lempicki, R.A., 2009. Systematic and integrative analysis of large gene lists using DAVID bioinformatics resources. Nat. Protoc. 4 (1), 44–57. http://dx.doi.org/10.1038/nprot.2008.211.

Kerpedjieva, S.S., Kim, D.S., Barbeau, D.J., Tamama, K., 2012. EGFR ligands drive multipotential stromal cells to produce multiple growth factors and cytokines via early growth response-1. Stem Cells Dev. 21 (13), 2541–2551. http://dx.doi.org/10.1089/scd.2011.0711.

Kim, D.S., Kim, J.H., Lee, J.K., Choi, S.J., Kim, J.S., Jeun, S.S., Oh, W., Yang, Y.S., Chang, J.W., 2009. Overexpression of CXC chemokine receptors is required for the superior glioma-tracking property of umbilical cord blood-derived mesenchymal stem cells. Stem Cells Dev. 18 (3), 511–519. http://dx.doi.org/10.1089/scd.2008.0050.

Lee, Y.S., Won, K.J., Park, S.W., Lee, H.W., Kim, B., Kim, J.H., Kim, D.K., 2012. Mesenchymal stem cells regulate the proliferation of T cells via the growth-related oncogene/CXC chemokine receptor, CXCR2. Cell. Immunol. 279 (1), 1–11. http://dx.doi.org/10.1016/j.cellimm.2012.08.002.

Lemons, J.M., Feng, X.J., Bennett, B.D., Legesse-Miller, A., Johnson, E.L., Raitman, I., Pollina, E.A., Rabitz, H.A., Rabinowitz, J.D., Coller, H.A., 2010. Quiescent fibroblasts exhibit high metabolic activity. PLoS Biol. 8 (10), e1000514. http://dx.doi.org/10.1371/journal.pbio.1000514.

Li, H., Ghazanfari, R., Zacharaki, D., Ditzel, N., Isern, J., Ekblom, M., Mendez-Ferrer, S., Kassem, M., Scheding, S., 2014. Low/negative expression of PDGFR-alpha identifies the candidate primary mesenchymal stromal cells in adult human bone marrow. Stem Cell Rep. 3 (6), 965–974. http://dx.doi.org/10.1016/j.stemcr.2014.09.018.

Macpherson, I., Montagnier, L., 1964. Agar suspension culture for the selective assay of cells transformed by polyoma virus. Virology 23, 291–294.

Marrony, S., Bassilana, F., Seuwen, K., Keller, H., 2003. Bone morphogenetic protein 2 induces placental growth factor in mesenchymal stem cells. Bone 33 (3), 426–433.

Matsumoto, R., Omura, T., Yoshiyama, M., Hayashi, T., Inamoto, S., Koh, K.R., Ohta, K., Izumi, Y., Nakamura, Y., Akioka, K., Kitaura, Y., Takeuchi, K., Yoshikawa, J., 2005. Vascular endothelial growth factor-expressing mesenchymal stem cell transplantation for the treatment of acute myocardial infarction. Arterioscler. Thromb. Vasc. Biol. 25 (6), 1168–1173. http://dx.doi.org/10.1161/01.ATV.0000165696.25680.ce.

Mendelsohn, A.R., Larrick, J.W., 2016. Rejuvenating muscle stem cell function: restoring quiescence and overcoming senescence. Rejuvenation Res. 19 (2), 182–186. http://dx.doi.org/10.1089/rej.2016.1829.

Milasincic, D.J., Dhawan, J., Farmer, S.R., 1996. Anchorage-dependent control of muscle-specific gene expression in C2C12 mouse myoblasts. In Vitro Cell Dev. Biol. Anim. 32 (2), 90–99.

Morikawa, S., Mabuchi, Y., Kubota, Y., Nagai, Y., Niibe, K., Hiratsu, E., Suzuki, S., Miyauchi-Hara, C., Nagoshi, N., Sunabori, T., Shimmura, S., Miyawaki, A., Nakagawa, T., Suda, T., Okano, H., Matsuzaki, Y., 2009. Prospective identification, isolation, and systemic transplantation of multipotent mesenchymal stem cells in murine bone marrow. J. Exp. Med. 206 (11), 2483–2496. http://dx.doi.org/10.1084/jem.20091046.

Mourikis, P., Sambasivan, R., Castel, D., Rocheteau, P., Bizzarro, V., Tajbakhsh, S., 2012. A critical requirement for notch signaling in maintenance of the quiescent skeletal muscle stem cell state. Stem Cells 30 (2), 243–252. http://dx.doi.org/10.1002/stem.775.

Nasef, A., Mazurier, C., Bouchet, S., Francois, S., Chapel, A., Thierry, D., Gorin, N.C., Fouillard, L., 2008. Leukemia inhibitory factor: role in human mesenchymal stem cells mediated immunosuppression. Cell. Immunol. 253 (1–2), 16–22. http://dx.doi.org/10.1016/j.cellimm.2008.06.002.

Ortiz, L.A., Dutreil, M., Fattman, C., Pandey, A.C., Torres, G., Go, K., Phinney, D.G., 2007. Interleukin 1 receptor antagonist mediates the antiinflammatory and antifibrotic effect of mesenchymal stem cells during lung injury. Proc. Natl. Acad. Sci. U. S. A. 104 (26), 11002–11007. http://dx.doi.org/10.1073/pnas.0704421104.

Oskowitz, A., McFerrin, H., Gutschow, M., Carter, M.L., Pochampally, R., 2011. Serum-deprived human multipotent mesenchymal stromal cells (MSCs) are highly angiogenic. Stem Cell Res. 6 (3), 215–225. http://dx.doi.org/10.1016/j.scr.2011.01.004.

Pallafacchina, G., Francois, S., Regnault, B., Czarny, B., Dive, V., Cumano, A., Montarras, D., Buckingham, M., 2010. An adult tissue-specific stem cell in its niche: a gene profiling analysis of in vivo quiescent and activated muscle satellite cells. Stem Cell Res. 4 (2), 77–91. http://dx.doi.org/10.1016/j.scr.2009.10.003.

Pardee, A.B., 1974. A restriction point for control of normal animal cell proliferation. Proc. Natl. Acad. Sci. U. S. A. 71 (4), 1286–1290.

Peiffer, I., Eid, P., Barbet, R., Li, M.L., Oostendorp, R.A., Haydont, V., Monier, M.N., Milon, L., Fortunel, N., Charbord, P., Tovey, M., Hatzfeld, J., Hatzfeld, A., 2007. A sub-population of high proliferative potential-quiescent human mesenchymal stem cells is under the reversible control of interferon alpha/beta. Leukemia 21 (4), 714–724. http://dx.doi.org/10.1038/sj.leu.2404589.

Pelham Jr., R.J., Wang, Y., 1997. Cell locomotion and focal adhesions are regulated by substrate flexibility. Proc. Natl. Acad. Sci. U. S. A. 94 (25), 13661–13665.

Peng, Y., Kang, Q., Luo, Q., Jiang, W., Si, W., Liu, B.A., Luu, H.H., Park, J.K., Li, X., Luo, J., Montag, A.G., Haydon, R.C., He, T.C., 2004. Inhibitor of DNA binding/differentiation helix-loop-helix proteins mediate bone morphogenetic protein-induced osteoblast differentiation of mesenchymal stem cells. J. Biol. Chem. 279 (31), 32941–32949. http://dx.doi.org/10.1074/jbc.M403344200.

Philips, A., Huet, X., Plet, A., Rech, J., Vie, A., Blanchard, J.M., 1999. Anchorage-dependent expression of cyclin A in primary cells requires a negative DNA regulatory element and a functional Rb. Oncogene 18 (10), 1819–1825. http://dx.doi.org/10.1038/sj.onc.1202530.

Post, S., Abdallah, B.M., Bentzon, J.F., Kassem, M., 2008. Demonstration of the presence of independent pre-osteoblastic and pre-adipocytic cell populations in bone marrow-derived mesenchymal stem cells. Bone 43 (1), 32–39. http://dx.doi.org/10.1016/j.bone.2008.03.011.

Reinhart-King, C.A., Dembo, M., Hammer, D.A., 2008. Cell-cell mechanical communication through compliant substrates. Biophys. J. 95 (12), 6044–6051. http://dx.doi.org/10.1529/biophysj.107.127662.

Rumman, M., Dhawan, J., Kassem, M., 2015. Concise review: quiescence in adult stem cells: biological significance and relevance to tissue regeneration. Stem Cells 33 (10), 2903–2912. http://dx.doi.org/10.1002/stem.2056.

Sachidanandan, C., Sambasivan, R., Dhawan, J., 2002. Tristetraprolin and LPS-inducible CXC chemokine are rapidly induced in presumptive satellite cells in response to skeletal muscle injury. J. Cell Sci. 115 (Pt 13), 2701–2712.

Sage, J., Mulligan, G.J., Attardi, L.D., Miller, A., Chen, S., Williams, B., Theodorou, E., Jacks, T., 2000. Targeted disruption of the three Rb-related genes leads to loss of G(1) control and immortalization. Genes Dev. 14 (23), 3037–3050.

Sammons, J., Ahmed, N., El-Sheemy, M., Hassan, H.T., 2004. The role of BMP-6, IL-6, and BMP-4 in mesenchymal stem cell-dependent bone development: effects on osteoblastic differentiation induced by parathyroid hormone and vitamin D(3). Stem Cells Dev. 13 (3), 273–280. http://dx.doi.org/10.1089/154732804323099208.

Sellathurai, J., Cheedipudi, S., Dhawan, J., Schroder, H.D., 2013. A novel in vitro model for studying quiescence and activation of primary isolated human myoblasts. PLoS One 8 (5), e64067. http://dx.doi.org/10.1371/journal.pone.0064067.

Shyh-Chang, N., Daley, G.Q., Cantley, L.C., 2013. Stem cell metabolism in tissue development and aging. Development 140 (12), 2535–2547. http://dx.doi.org/10.1242/dev.091777.

Simonsen, J.L., Rosada, C., Serakinci, N., Justesen, J., Stenderup, K., Rattan, S.I., Jensen, T.G., Kassem, M., 2002. Telomerase expression extends the proliferative life-span and maintains the osteogenic potential of human bone marrow stromal cells. Nat. Biotechnol. 20 (6), 592–596. http://dx.doi.org/10.1038/nbt0602-592.

Soleimani, M., Nadri, S., 2009. A protocol for isolation and culture of mesenchymal stem cells from mouse bone marrow. Nat. Protoc. 4 (1), 102–106. http://dx.doi.org/10.1038/nprot.2008.221.

Sousa-Victor, P., Gutarra, S., Garcia-Prat, L., Rodriguez-Ubreva, J., Ortet, L., Ruiz-Bonilla, V., Jardi, M., Ballestar, E., Gonzalez, S., Serrano, A.L., Perdiguero, E., Munoz-Canoves, P., 2014. Geriatric muscle stem cells switch reversible quiescence into senescence. Nature 506 (7488), 316–321. http://dx.doi.org/10.1038/nature13013.

Subramaniam, S., Sreenivas, P., Cheedipudi, S., Reddy, V.R., Shashidhara, L.S., Chilukoti, R.K., Mylavarapu, M., Dhawan, J., 2013. Distinct transcriptional networks in quiescent myoblasts: a role for Wnt signaling in reversible vs. irreversible arrest. PLoS One 8 (6), e65097. http://dx.doi.org/10.1371/journal.pone.0065097.

Tse, J.R., Engler, A.J., 2010. Preparation of hydrogel substrates with tunable mechanical properties. Curr. Protoc. Cell Biol. http://dx.doi.org/10.1002/0471143030.cb1016s47. (Chapter 10, Unit 10 16).

Twine, N.A., Harkness, L., Adjaye, J., Aldahmash, A., Wilkins, M., Kassem, M., 2018. Molecular phenotyping of telomerized human bone marrow skeletal stem cells reveals a genetic program of enhanced proliferation and maintenance of differentiation responses. JBMR Plus. http://dx.doi.org/10.1002/jbm4.10050.

Venugopal, B., Mogha, P., Dhawan, J., Majumder, A., 2018. Cell density overrides the effect of substrate stiffness on human mesenchymal stem cells' morphology and proliferation. Biomater Sci. http://dx.doi.org/10.1039/c7bm00853h.

Vizoso, F.J., Eiro, N., Cid, S., Schneider, J., Perez-Fernandez, R., 2017. Mesenchymal stem cell secretome: toward cell-free therapeutic strategies in regenerative medicine. Int. J. Mol. Sci. 18 (9). http://dx.doi.org/10.3390/ijms18091852.

Wang, M., Zhang, X., Xiong, X.I., Yang, Z., Li, P., Wang, J., Sun, Y.U., Yang, Z., Hoffman, R.M., 2016. Bone marrow mesenchymal stem cells reverse liver damage in a carbon tetrachloride-induced mouse model of chronic liver injury. In Vivo 30 (3), 187–193.

Winer, J.P., Janmey, P.A., McCormick, M.E., Funaki, M., 2009. Bone marrow-derived human mesenchymal stem cells become quiescent on soft substrates but remain responsive to chemical or mechanical stimuli. Tissue Eng. Part A 15 (1), 147–154. http://dx.doi.org/10.1089/ten.tea.2007.0388.

Witkowska-Zimny, M., Walenko, K., Wrobel, E., Mrowka, P., Mikulska, A., Przybylski, J., 2013. Effect of substrate stiffness on the osteogenic differentiation of bone marrow stem cells and bone-derived cells. Cell Biol. Int. 37 (6), 608–616. http://dx.doi.org/10.1002/cbin.10078.

Yeung, T., Georges, P.C., Flanagan, L.A., Marg, B., Ortiz, M., Funaki, M., Zahir, N., Ming, W., Weaver, V., Janmey, P.A., 2005. Effects of substrate stiffness on cell morphology, cytoskeletal structure, and adhesion. Cell Motil. Cytoskeleton 60 (1), 24–34. http://dx.doi.org/10.1002/cm.20041.

Zaher, W., Harkness, L., Jafari, A., Kassem, M., 2014. An update of human mesenchymal stem cell biology and their clinical uses. Arch. Toxicol. 88 (5), 1069–1082. http://dx.doi.org/10.1007/s00204-014-1232-8.

Zismanov, V., Chichkov, V., Colangelo, V., Jamet, S., Wang, S., Syme, A., Koromilas, A.E., Crist, C., 2016. Phosphorylation of eIF2alpha is a translational control mechanism regulating muscle stem cell quiescence and self-renewal. Cell Stem Cell 18 (1), 79–90. http://dx.doi.org/10.1016/j.stem.2015.09.020.